EDN: NKANAC
УДК 519.3

Analysis of the Influence of Porosity and Non-Uniform Polarization of Piezoelectric Ceramics on the Efficiency of a Bridge Transducer as Sensor and Actuator

Andrey V. Nasedkin*
Anna A. Nasedkina†
Southern Federal University
Rostov on Don, Russian Federation

Received 10.09.2024, received in revised form 22.10.2024, accepted 26.12.2024

Abstract. Flexible piezoelectric transducers, and the transducers with bridge shaped end-caps in particular, have found wide application as acoustic emitters and energy harvesting devices. In this paper, we investigate the possibilities of using porous piezoceramics as an active element of a bridge transducer. Particular attention is paid to taking into account the non-uniform polarization of porous piezoceramics with the use of simplified models. A finite element analysis of the bridge piezoelectric transducer under steady-state oscillations is performed in resonant and non-resonant modes of its operation. It is found that the use of porous piezoceramics increases the efficiency of the transducer during oscillations near the first frequency of electrical antiresonance.

Keywords: electroelasticity, bridge piezoelectric transducer, porous piezoceramics, non-uniform polarization, resonant frequency, sensor, actuator, finite element method.

Citation: A.V. Nasedkin, A.A. Nasedkina, Analysis of the Influence of Porosity and Non-Uniform Polarization of Piezoelectric Ceramics on the Efficiency of a Bridge Transducer as Sensor and Actuator, J. Sib. Fed. Univ. Math. Phys., 2025, 18(2), 218–228. EDN: NKANAC.

Piezoelectric transducers are widely used in various technical devices. In order to improve their efficiency for specific applications, it is necessary to ensure high values of individual parameters or quality factors. This paper presents the results of the study of a piezoelectric transducer consisting of a piezoelectric ceramic plate polarized by thickness with two metal bridge-shaped end-caps. Here, for the initial device we consider a bridge piezoelectric transducer with a plate made of dense piezoelectric ceramics, which was previously studied in [1].

As modern research has shown, bridge transducers can be effectively used as part of energy havesting devices [2–5], current sensors [6] and emitters. Various types of bridge transducers have been analyzed in [7–11], etc. Original approaches for optimizing the bridge transducer design were proposed in [12, 13].

Another type of piezoelectric transducers similar to bridge transducers are axisymmetric transducers, which are also called Cymbal Transducers, because their end-caps are shaped like cymbal plates. Cymbal transducers have been studied in more details than bridge transducers. In practical applications they are actively used as sensors or sources of renewable energy [2, 4], as well as actuators or emitters [14].

*avnasedkin@sfedu.ru https://orcid.org/0000-0002-3883-2799
†aanasedkina@sfedu.ru https://orcid.org/0000-0003-1258-4886

Improvement of the characteristics of piezoelectric devices can be achieved by using piezoelectric composites as active materials of transducers. In particular, it is possible to use porous piezoceramics, that are more compliant and have lower acoustic impedance, but at the same time have some high electromechanical coupling coefficients with the values close to those of dense piezoceramics. However, for porous piezoceramics, the influence of the inhomogeneity of the polarization field in the vicinity of the pores on its effective properties has not been sufficiently studied yet. Precise application of porous piezoceramics also requires an account of the porosity structure microfeatures and optimization of individual material constants, geometry and boundary conditions for a specific device.

Some of the above issues were investigated in [16–18] for Cymbal transducers with a disk made of porous piezoceramics. In this paper, the efficiency of using porous piezoceramic materials for a bridge piezoelectric transducer is studied in a similar manner. For the active element materials we consider conventional dense piezoceramics and porous piezoceramics PZT-4 with the effective moduli calculated using uniform and non-uniform polarization models [19].

1. General problem statement

1.1. Geometrical and physical data

Let us consider a bridge transducer with the geometric parameters adopted in [1]. This transducer consists of a piezoceramic plate of length $L = 12.7$ (mm), width $b = 12.7$ (mm), and thickness $h_p = 1$ (mm). The end surfaces of the plate relative to its thickness are covered with electrodes, and the piezoceramic material of the plate is polarized by thickness. On some of the end surfaces there are metal bridge caps of width b equal to the width of the plate. Each cover has a thickness $h_c = 0.3$ (mm) and a maximum lift height $h_m = 0.35$ (mm). The maximum lift surfaces are flat and have length $l_m = 3$ (mm), and the sections of the bridge caps connected to the plate have lengths $l_c = 1.85$ (mm).

This geometry, as well as the external influences and fixing conditions adopted further, make it possible to consider one fourth of the device with the corresponding symmetry conditions during finite element modeling. In Fig. 1, the symmetry surface of the fourth part of the transducer is shown in the Oxz plane, related to the Cartesian coordinate system $Oxyz$. Along the Oy axis, all elements of the device quarter occupy the region $-b/2 \leqslant y \leqslant 0$.

For metal overlays, we will accept the properties of brass as an elastic isotropic material with density of $\rho_m = 8400$ (kg/m^3), Young's modulus $E_m = 9.5 \cdot 10^{10}$ (N/m^2) and Poisson's ratio $\nu_m = 0.35$.

The central plate of the transducer is made of PZT-4 piezoceramics with the main direction of polarization along the thickness. For PZT-4 piezoceramics, we will accept different material properties. We will consider dense piezoceramics with stiffness moduli $c^E_{\alpha\beta}$, piezoelectric moduli $e_{i\beta}$ and dielectric permittivity coefficients ε^S_{ij}, as well as porous piezoceramics with effective stiffness moduli $c^{E\,\mathrm{eff}}_{\alpha\beta}$, effective piezomoduli $e^{\mathrm{eff}}_{i\beta}$ and effective permittivity moduli $\varepsilon^{S\,\mathrm{eff}}_{ij}$. Here and below, Greek indices may vary from 1 to 6, and Latin indices vary from 1 to 3: $\alpha, \beta = 1, 2, \ldots, 6$, $i, j = 1, 2, 3$. For the moduli of dense piezoceramics, we use the standard notations of the theory of piezoelectricity (electroelasticity) [20]. In particular, the superscripts indicate at what constant fields the material moduli of electroelasticity used in various constitutive relations were determined. Thus, the superscript E means the constancy of the electric field, D means the constancy of the electric induction field, S means the constancy of the strain fields, and T means

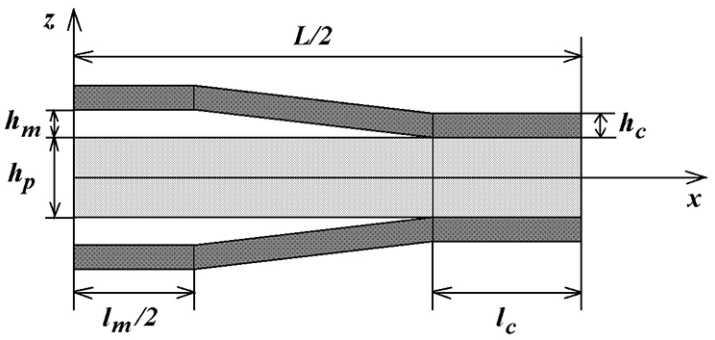

Fig. 1. Geometry of the longitudinal cross-section of the bridge transducer for $x \geqslant 0$, $y = 0$

the constancy of the mechanical stress fields.

The moduli of the porous piezoceramics were determined from the initial moduli of the dense piezoceramics as a result of numerical calculations using the effective moduli method in the ANSYS finite element package. For this purpose, a cubic representative volume V was used, regularly divided into n_e^3 piezoelectric cubic finite elements, where n_e is the number of finite elements along a separate axis of the Cartesian coordinate system. Based on a given percentage of porosity p, $n_p = [pn_e^3/100]$ elements were randomly selected from among these elements, where [...] is the integer part of the number, and these elements were assigned the material properties of the pores, i.e. negligibly small elastic stiffnesses, piezomoduli and permittivities equal to the permittivity of vacuum $\varepsilon_0 = 8.85 \cdot 10^{-12}$ (F/m). The number n_e was determined by the convergence of the results of calculations of effective moduli, and as a result of numerical experiments it was taken to be equal to 45.

Four sets of material properties were used to calculate the piezoelectric transducer. In the basic variant (variant 0), the piezoelectric ceramics were assumed solid and uniformly polarized along the Oz axis. In variant 1, porous piezoceramics were considered with moduli calculated for a piezoelectric ceramic matrix uniformly polarized along the Oz axis.

In variant 2, the finite element method was used to solve the problem of dielectric electrostatics, simulating the polarization process of porous piezoceramics in a simplified formulation, and the polarization vectors $\mathbf{P}^{em}$ were found for each finite element with number m. Then, the heterogeneity of the properties of the piezoceramic matrix was determined by element coordinate systems in which the z^{em} axis for individual finite element with number m was directed along the vector $\mathbf{P}^{em}$. In this variant, the moduli were considered equal to the moduli of dense ceramics $c^E_{\alpha\beta}$, $e_{i\beta}$, ε^S_{ij}, but in the elementcoordinate system $Ox^{em}y^{em}z^{em}$, and then they were recalculated to the values $c^{Eem}_{r\alpha\beta}$, $e^{em}_{ri\beta}$, ε^{Sem}_{rij} in the global coordinate system in accordance with the formulas for transforming the components of the tensors when rotating the coordinate systems.

Finally, in the most realistic version 3, the properties of the piezoceramic matrix for each finite element varied linearly between the corresponding values of the properties of unpolarized ceramics ($s^{np}_{\alpha\beta}$, $d^{np}_{i\beta} = 0$, ε^{np}_{ij}) and the properties of polarized ceramics $s^{Eem}_{r\alpha\beta}$, $d^{em}_{ri\beta}$, ε^{Tem}_{ij}, in accordance with the formulas

$$s^{Eem}_{\alpha\beta} = (1-\chi_p)s^{np}_{\alpha\beta} + \chi_p s^{Eem}_{r\alpha\beta}, \quad d^{em}_{i\beta} = \chi_p d^{em}_{ri\beta}, \quad \varepsilon^{Tem}_{ij} = (1-\chi_p)\varepsilon^{np}_{ij} + \chi_p \varepsilon^{Tem}_{rij}, \tag{1}$$

$$\chi_p = \begin{cases} |\mathbf{P}^{em}|/P_{sat} & |\mathbf{P}^{em}| \leqslant \kappa_p P_{sat}, \\ \kappa_p & |\mathbf{P}^{em}| > \kappa_p P_{sat}. \end{cases} \tag{2}$$

Here $s^{np}_{\alpha\beta}$, $s^{Eem}_{r\alpha\beta}$ are the components of the compliance matrices of unpolarized and polarized ceramics, which are inverse to the corresponding stiffness matrices with components $c^{np}_{\alpha\beta}$ and $c^{Eem}_{r\alpha\beta}$, $\varepsilon^{np}_{ij} = \varepsilon^{np}$, $d^{em}_{ri\beta} = e^{em}_{ri\zeta} s^{Eem}_{r\zeta\beta}$, $\varepsilon^{Tem}_{rij} = \varepsilon^{Sem}_{rij} + d^{em}_{ri\zeta} e^{em}_{rj\zeta}$, $P_{sat} = (\varepsilon^{np} - \varepsilon_0) E_c$, E_c is the value of the polarization field from the electrostatics problem simulating the polarization process, κ_p is the parameter determining the possibility of "superpolarization", which we set equal to 1.2. Further, after finding the moduli $s^{Eem}_{r\alpha\beta}$, $d^{em}_{ri\beta}$, ε^{Tem}_{rij} from (1), (2), it is easy to go to the moduli $s^{Eem}_{r\alpha\beta}$, $d^{em}_{ri\beta}$, ε^{Tem}_{rij} from the main calculation constitutive relations using the corresponding formulas.

The technique for finding effective moduli from solutions of static boundary value problems of electroelasticity with linear essential boundary conditions for displacements and electric potential for homogenous polarized piezoceramics is well known and has been described in many papers. For non-uniformly polarized piezoceramics, we relied on the approaches presented in [19]. However, we supplemented the model $s^E d\varepsilon^T$ with (1), (2) when finding the moduli of unpolarized ceramics by Hill's averaging not only the original moduli $c^E_{\alpha\beta}$, ε^S_{ij}, but also the moduli $c^D_{\alpha\beta}$, ε^T_{ij}, as well as by restricting the value of κ_p in the "superpolarization" model. The results of calculations of the complete set of effective moduli of porous piezoceramics PZT-4 for three variants considering heterogeneities are given in Tab. 1.

Table 1. Initial moduli of dense piezoceramics PZT-4 and effective moduli of porous piezoceramics for three polarization models ($c^{E\,\mathrm{eff}}_{\alpha\beta} \cdot 10^{10}$ in N/m^2, $e_{i\beta}$ in C/m^2, $\tilde{\varepsilon}^{S\,\mathrm{eff}}_{ii} = \varepsilon^{S\,\mathrm{eff}}_{ii}/\varepsilon_0$)

No.	p (%)	$c^{E\,\mathrm{eff}}_{11}$	$c^{E\,\mathrm{eff}}_{12}$	$c^{E\,\mathrm{eff}}_{13}$	$c^{E\,\mathrm{eff}}_{33}$	$c^{E\,\mathrm{eff}}_{44}$	e^{eff}_{31}	e^{eff}_{33}	e^{eff}_{15}	$\tilde{\varepsilon}^{S\,\mathrm{eff}}_{11}$	$\tilde{\varepsilon}^{S\,\mathrm{eff}}_{33}$
0	0	13.90	7.78	7.43	11.5	2.56	–5.2	15.1	12.7	730	635
1	10	11.69	6.32	5.98	9.57	2.22	–4.24	13.41	10.92	657.5	0.85
1	20	9.53	4.92	4.61	7.73	1.88	–3.30	11.68	9.15	583.8	565.8
1	30	7.45	3.61	3.34	5.95	1.55	–2.40	9.86	7.40	510.0	427.4
1	40	5.47	2.45	2.24	4.35	1.21	–1.56	7.98	5.66	431.2	358.5
1	50	3.69	1.49	1.34	2.88	0.88	–0.83	5.89	3.99	352.3	288.4
2	10	11.69	6.32	5.95	9.54	2.22	–4.12	13.45	10.90	653.4	566.3
2	20	9.56	4.92	4.56	7.66	1.87	–3.07	11.74	9.10	576.0	497.5
2	30	7.41	3.60	3.26	5.87	1.53	–2.04	9.96	7.30	496.9	428.5
2	40	5.42	2.42	2.14	4.26	1.19	–1.14	8.06	5.55	416.2	359.2
2	50	3.64	1.47	1.26	2.84	0.86	–0.40	6.02	3.88	333.8	288.9
3	10	11.66	6.28	5.96	9.56	2.23	–3.83	13.53	10.69	666.6	567.9
3	20	9.48	4.85	4.55	7.69	1.90	–2.60	11.78	8.71	602.4	504.0
3	30	7.34	3.50	3.26	5.94	1.57	–1.56	9.92	6.79	531.0	441.3
3	40	5.36	2.31	2.13	4.32	1.24	–0.72	7.86	4.95	455.9	376.8
3	50	3.58	1.37	1.25	2.91	0.90	–0.13	5.66	3.26	371.5	308.9

As can be seen from Tab. 1, polarization models have the least effect on the effective elastic moduli, and the greatest effect on the effective piezoelectric moduli, especially on the transverse piezoelectric modulus e^{eff}_{31}.

1.2. System of equations for harmonic vibrations

For a bridge transducer, we will use the equations of electroelasticity, which in the steady-state oscillation mode $\exp(j\omega t)$ with frequency $f = \omega/(2\pi)$ for the amplitude values of the displacements $u_k(\mathbf{x})$ and the electric potential $\varphi(\mathbf{x})$ we will represent in the form

$$\sigma_{kl,l} + \rho\omega^2 u_k = 0, \quad D_{k,k} = 0, \tag{3}$$

$$T_\alpha = (1 + jQ_d^{-1})c^E_{\alpha\beta}S_\beta - e_{k\alpha}E_k, \quad D_k = e_{k\beta}S_\beta + \varepsilon^S_{kl}E_l, \tag{4}$$

$$\varepsilon_{kl} = (u_{k,l} + u_{l,k})/2, \quad E_k = -\varphi_{,k}. \tag{5}$$

Here σ_{kl} are the components of the stress tensor; ε_{kl} are the components of the strain tensor; $\{T_1, T_2, T_3, T_4, T_5, T_6\} = \{\sigma_{11}, \sigma_{22}, \sigma_{33}, \sigma_{23}, \sigma_{13}, \sigma_{12}\}$, $\{S_1, S_2, S_3, S_4, S_5, S_6\} = \{\varepsilon_{11}, \varepsilon_{22}, \varepsilon_{33}, 2\varepsilon_{23}, 2\varepsilon_{13}, 2\varepsilon_{12}\}$; D_k are the components of the electric induction vector; E_k are the components of the electric field strength vector; ρ is the density; Q_d is the mechanical quality factor for the frequency-independent method of accounting for damping; j is the imaginary unit.

For porous piezoceramics in (3) the density must be recalculated considering the porosity, and in (4) it is necessary to use effective moduli.

Equations (3)–(5) for mechanical fields with $e_{k\beta} = 0$ are equations of elasticity theory with the same method of taking into account damping, and therefore they also describe the vibrations of elastic end-caps in a piezoelectric transducer.

Next, we will consider two types of bridge transducers for different applications. Transducer type A is focused on the problems of energy harvesting from mechanical low-frequency pressures, and transducer type B must operate in resonant mode and generate acoustic waves in the external medium under electrical effects. The problems for these two types of transducers differ in the fixing conditions and external influences.

2. Bridge transducer type A

In the transducer of type A the lower plateau $z = -H$ ($H = h_c + h_m + h_p/2$) was rigidly fixed, and the upper plateau $z = H$ was subjected to pressure oscillating with frequency f of amplitude $p = F/(l_m b)$, where F is the total force. The electroded boundaries of the piezoceramic plate are equipotential, i.e. $\varphi = \Phi_i$, $z = \pm h_p/2$, where the electric potential values Φ_i are constant for each of the two electrodes. These electrodes in transducer A were connected by an external electric circuit with resistance R. The overall quality factor Q_d of the entire device was taken to be equal to 1000.

For the transducer A, the steady-state oscillation mode in the non-resonant frequency range $f \in (0, 2]$ (Hz) was considered, which corresponds to its use as an energy harvesting device. When the transducer was loaded with pressure with a total force $F = 800$ (N), the maximum induced electric potential difference ΔV between the electrodes was determined when they were connected by an electric circuit with a resistance $R = 2$ (kΩ). The results of calculating problem (3)–(5) for the induced electric potential difference and axial displacement at the upper central point of the transducer $\{0, 0, H\}$ depending on the porosity are shown in Fig. 2. Here and below, curves with numbers 1–3 are constructed for porous piezoceramics with effective moduli from the corresponding variants 1–3 of the polarization models.

As can be seen from Fig. 2 (a), the use of porous piezoceramics in the transducer plate with bridge end-caps demonstrates the worst properties to preserve energy compared to dense. Accounting for the heterogeneity of the polarization field slightly reduces the values of the induced difference in the electrical potential compared to the model of homogeneous polarization. Meanwhile, the amplitudes of axial displacements $|u_z|$ at the upper center point of the transducer $\{0, 0, H\}$ increase with the growth of porosity (Fig. 2 (b)), which is quite natural, since porous material is more supple than the corresponding solid. Polarization models practically do not affect the amplitude of maximum axial displacements.

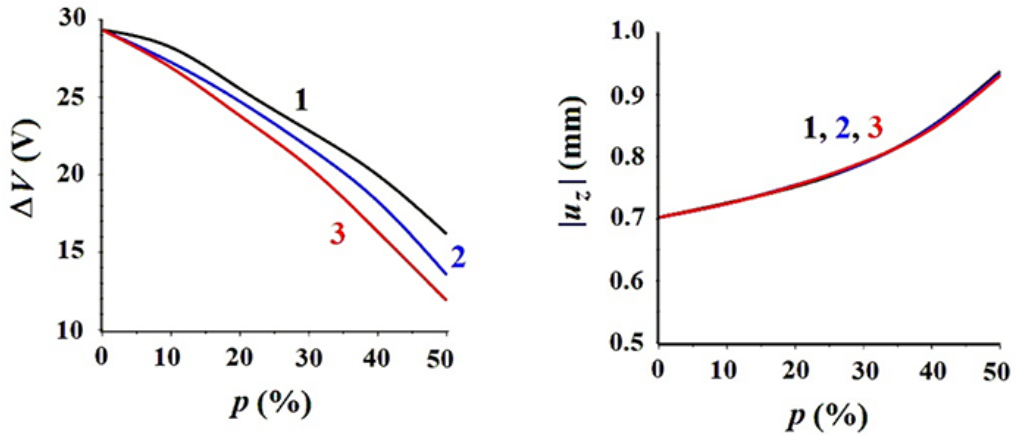

(a) (b)

Fig. 2. Induced electric potential difference (a) and axial displacement at the top central point (b) for transducer A made from different variants of porous piezoceramics

3. Bridge transducer type B

In the transducer B almost all external surfaces are considered stress-free, but at the extreme edges of the plate $x = L/2$, $y = \pm h_p/2$ the axial displacement $u_z = 0$ is fixed. We will consider two cases of generating acoustic vibrations in the transducer. In the first case, the oscillations are generated by applying a difference in electrical potentials $\Delta V = |\Phi_2 - \Phi_1|$ between the electrodes $\Gamma_{\varphi 2} = \{z = h_p/2\}$ and $\Gamma_{\varphi 1} = \{z = -h_p/2\}$. In the second case, the external influence is the electric current I or the charge $Q = -\int\limits_{\Gamma_{\varphi 2}} D_3\, d\Gamma$ on one electrode, for example, on the electrode $\Gamma_{\varphi 2}$, with zero potential $\Phi_1 = 0$ on the other electrode, for example, on $\Gamma_{\varphi 1}$. (Here $I = \pm j\omega Q$, and since we are considering problems for the amplitude values of displacements and electric potential, the factor $\exp(j\omega t)$ is omitted everywhere.)

The transducer of type B is designed to operate as an emitter of acoustic waves into the external medium when it is electrically excited. The investigations of its gain-frequency characteristics in the steady-state oscillation mode were carried out in two stages. At the first stage, problems were solved in ANSYS to determine the electrically active first frequencies of electrical resonances f_{r1} and antiresonances f_{r2}, and at the second stage, the amplitude-frequency characteristics were constructed based on the results of calculations obtained on intervals including the corresponding frequencies of electrical resonances and antiresonances.

Note that the frequencies of electrical resonances f_{rk} and the frequencies of electrical antiresonances f_{ak} are the resonance frequencies of the device and can lead to classical resonance phenomena under various electrical influences: the difference in electrical potentials or current.

Namely, if we consider the specification of potential difference $\Delta V \exp(i2\pi ft)$ on electrode surfaces with the frequency $f = \omega/(2\pi)$ and with fixed amplitude ΔV, then in such problem at electric resonance frequencies f_{rk}, $k = 1, 2, \ldots$, in the absence of damping, resonance phenomena may occur for displacements, electric current amplitudes I and electric admittance $Y = I/(\Delta V)$:

$$|I| \to \infty, \quad |Y| \to \infty, \quad f \to f_{rk}. \tag{6}$$

Another option is to excite oscillations by a harmonically changing electric current

$I\exp(i2\pi ft)$ with a fixed amplitude I (electric charge $Q = iI/(2\pi f)$. In such a problem, resonance phenomena can be observed at the frequencies of electric antiresonance f_{ak} for displacements, amplitudes of the electrical potential difference ΔV and electric resistance (impedance) $Z = \Delta V/I = Y^{-1}$:

$$|\Delta V| \to \infty, \quad |Z| \to \infty, \quad f \to f_{ak}. \tag{7}$$

Our two cases of external electrical influences correspond exactly to the capabilities of the bridge transducer to operate at the frequencies of electrical resonances (6) and antiresonances (7). In modal analysis in ANSYS, we solve problems with homogeneous boundary conditions twice. First, we set zero potentials on both electrodes and find the eigenvalues, among which the frequencies of electrical resonances may be. Then we change the boundary conditions on one of the electrodes, making it free, i.e. with zero total charge. From this problem, we find the eigenvalues, the set of which contains the frequencies of electrical antiresonances. Comparing the two resulting sets and selecting electrically active frequencies with close ordinal numbers, but differing from each other, we find the desired frequencies of the first electrical resonances and antiresonances.

Conducting modal analysis allows us to construct amplitude-frequency characteristics more accurately, since the boundaries of frequency sub-intervals will be close to possible resonance frequencies (or equal to them, in problems without taking damping into account). For further analysis, we will select the amplitude-frequency characteristics of the axial displacement $|u_z|$ at the top central point $\{0, 0, H\}$, as well as the output charge or potential difference.

Some calculation results are shown in Figs. 3 and 4. Curve numbers 1–3 in these figures denote the same types of porous piezoceramics as in Fig. 2. Solid curves with numbers 1–3 are plotted for materials with a porosity of 40%, and dashed curves are plotted for materials with a porosity of 20%. Green curves with number 0 are plotted for the dense piezoceramics material PZT-4 (with zero porosity $p = 0$). The amplitude-frequency characteristics in Fig. 3 and in Fig. 4 are plotted for different electrical effects: Fig. 3 corresponds to the problem with a given oscillating potential difference with a modulus $\Delta V = 100$ (V), and Fig. 4 corresponds to the problem with a given electric charge $Q = -4.25 \cdot 10^{-8}$ (Ω) on one electrode with the second electrode grounded. The quality factor Q_d of the material of the metal end-caps was taken to be equal to 1000, and the quality factor of the piezoceramics was considered to be equal to 500.

The main results are presented in Fig. 3 (a) and 4 (a), which show the amplitude-frequency characteristics of the displacement at the central upper point of the transducer. Fig. 3 (b) and 4 (b) illustrate the resonance phenomena (6), (7). Thus, in the V-problem, for a given fixed amplitude of the potential difference ΔV, an increase in the amplitudes of the electric charge is observed at the first frequencies of electric resonance (Fig. 3 (b)), and in the Q-problem, for a given fixed amplitude of the electric charge Q, an increase in the amplitudes of the potential difference is observed at the first frequencies of electric antiresonance (Fig. 4 (b)).

As can be seen from Fig. 3 (a) and 4 (a), the porosity dependences of the maximum displacement amplitudes in these two problems are quite different. The models of inhomogeneity of porous piezoceramics also affect the values of the oscillation amplitudes, but not very significantly. When setting the potential difference (Fig. 3 (a)) the amplitudes of the axial displacement maxima at resonance frequencies decrease with increasing porosity. The dependences of the axial displacement maxima change significantly when the transducer oscillations are excited by an electric charge (Fig. 4 (a)). Here the displacement maxima increase with increasing porosity.

Note that in all cases at the first resonance frequencies, the axial displacements of the transducer in the central end regions are an order of magnitude greater than the longitudinal dis-

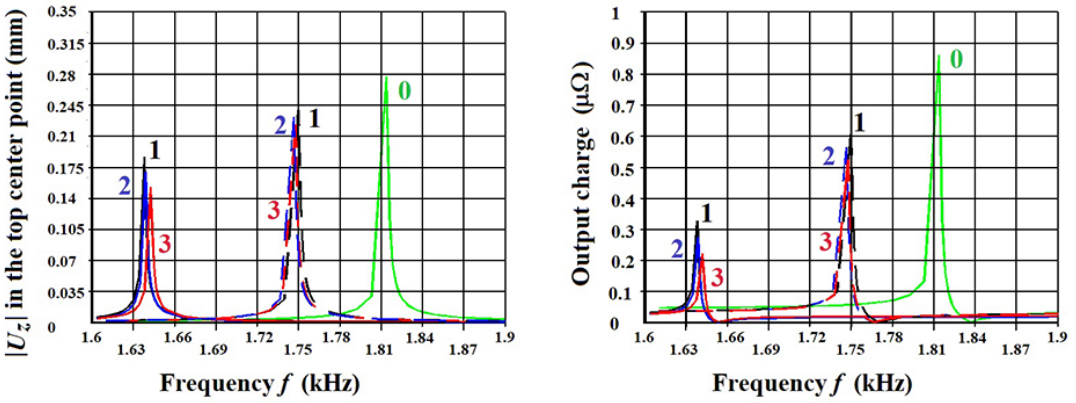

(a) (b)

Fig. 3. Displacements at the upper central point (a) and the output electric charge (b) in the V-problem under the action of a potential difference

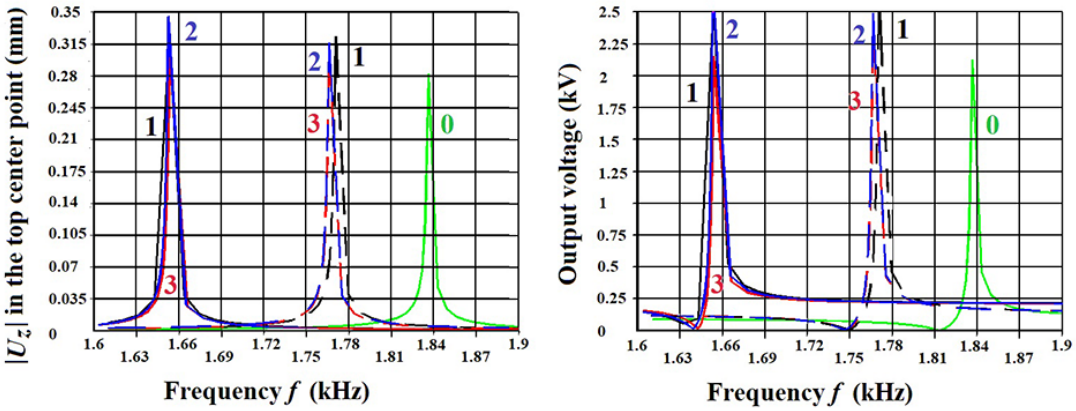

(a) (b)

Fig. 4. Displacements at the upper central point (a) and the output potential difference (b) in the Q-problem under the action of an electric charge

placements of its side surfaces. Thus, the bridge transducer at the first resonance frequency effectively generates axial oscillations. At the same time, calculations of the amplitude-frequency characteristics at a higher resonant frequency showed a lower efficiency of excitation of axial displacements. Nevertheless, in general, if we also take into account the lower acoustic impedance of porous piezoceramics compared to dense ones, we can conclude that the use of the considered porous piezoceramics as active materials for acoustic wave emitters is promising.

It can also be noted that the behavioral features of bridge transducers made of porous piezoceramics as sensors and actuators are similar to the behavioral features of the Symbol transducer [17, 18]. In [17, 18], porous piezoceramics with metallized surface pores were also considered, but non-uniform polarization models were not taken into account. For the porous Symbol transducer, in [17, 18], an advantage was found in using porous piezoceramics with metallized surface pores for energy harvesting and in the V-problem for actuator applications. Therefore, it

can be concluded that porous piezoceramics with metallized surface pores for similar applications will also be effective for a bridge transducer. However, the technological processes for creating such porous piezoceramics have not yet been fully developed.

Conclusion

Thus, here, a bridge piezoelectric transducer consisting of a piezoceramic plate with two bridge-like metal end-caps was investigated using computer modelling methods. The use of porous piezoceramics as the active material of the transducer and the consideration of various models of non-uniform polarization were analyzed.

Two types of bridge piezoelectric transducers are considered. The first transducer is intended for use as a "green energy" piezoelectric generator. It generated electric fields in the transducer under low-frequency mechanical influences. For this device, the use of porous ceramics showed lower efficiency of electromechanical conversion compared to dense ceramics.

The second type of transducer worked as an emitter of acoustic waves. It converted electrical influences near the first resonance frequency into mechanical vibrations. In this case, when the transducer was excited by the potential difference at the first frequencies of electrical resonances, qualitatively similar results were obtained for the use of porous piezoceramics as for the bridge piezogenerator. However, the bridge transducer made of porous piezoceramics showed its efficiency when working at the first antiresonance frequency when its vibrations were excited by electric current. It also turned out that considering the inhomogeneity of polarization of porous piezoceramics is essential for precision modeling of a bridge converter, but taking into account the inhomogeneity does not affect the qualitative characteristics.

This research was supported by the Russian Science Foundation, project no. 22-11-00302.

References

[1] L.Luo, Y.Tang, F.Wang, C.He, H.Luo, Displacement amplification and electric characteristics of modified rectangular cymbal transducers using electroactive materials, *Solid State Commun.*, **143**(2007), 321–325. DOI: 10.1016/j.ssc.2007.05.037

[2] H .Wang, A.Jasim, X.Chen, Energy harvesting technologies in roadway and bridge for different applications - A comprehensive review, *Appl. Energy.* **212**(2018), 1083–1094. DOI: 10.1016/j.apenergy.2017.12.125

[3] L.Yao, H.D.Zhao, Z.Y.Dong, Y.F.Sun, Y.F.Gao, Laboratory testing of piezoelectric Bridge transducers for asphalt pavement energy harvesting, *Key Eng. Mater.*, **492**(2012), 172–175. DOI: 10.4028/www.scientific.net/kem.492.172

[4] H.Zhao,L.Qin, J.Ling, A comparative analysis of piezoelectric transducers for harvesting energy from asphalt pavement, *J. Ceram. Soc. Jpn.*, **120**(2012), no. 1404, 317–323. DOI: 10.2109/jcersj2.120.317

[5] H.Zhao, J.Ling, J.Yu, Test and analysis of bridge transducers for harvesting energy from asphalt pavement , *Int. J. Transp. Sci. Technol.*, **4**(2015), no. 1, 17–28. DOI: 10.1260/2046-0430.4.1.17

[6] W.Hea, Y.Lu, C.Qu, J.Peng, A non-invasive electric current sensor employing a modified shear-mode cymbal transducer, *Sensors Actuat. A* , **241**(2016), 120–123 DOI: 10.1016/j.sna.2016.02.015

[7] A.Daniels, M.Zhu,.A.Tiwari, Design, analysis and testing of a piezoelectric flex transducer for harvesting biokinetic energy, *J. Phys.: Conf. Ser.*, **476**(2013), 012047. DOI: 10.1088/1742-6596/476/1/012047

[8] A.Jasim, H.Wang, G.Yesner, A.Safari, A.Maher, Optimized design of layered bridge transducer for piezoelectric energy harvesting from roadway, *Energy*, **141**(2017), 1133–1145. DOI: 10.1016/j.energy.2017.10.005

[9] Y.Kuang, A.Daniels, M.Zhu, A sandwiched piezoelectric transducer with flex end-caps for energy harvesting in large force environments, *J. Phys. D: Appl. Phys.* **50**(2017), 345501. DOI: 10.1088/1361-6463/aa7b28

[10] B.Ren, S.W.Or, X.Zhao, H.Luo, Energy harvesting using a modified rectangular cymbal transducer based on 0.71Pb $(Mg_{1/3}Nb_{2/3})$ O_3–0.29 $PbTiO_3$ single crystal, *J. Appl. Phys.*, **107**(2010), 034501. DOI: 10.1063/1.3296156

[11] G.Yesner, A.Jasim, H.Wang, B.Basily, A.Maher, A.Safari, Energy harvesting and evaluation of a novel piezoelectric bridge transducer , *Sensors Actuat. A*, **285**(2019), 348–354. DOI: 10.1016/j.sna.2018.11.013

[12] L.Luo, D.Liu, M.Zhu, J.Ye, Metamodel-assisted design optimization of piezoelectric flex transducer for maximal bio-kinetic energy conversion, *J. Intell. Mater. Syst. Struct.*, **28**(2017), no. 18, 2528–2538. DOI: 10.1177/1045389X17689943

[13] L.Luo, D.Liu, M.Zhu, Y.Liu, L.Ye, Maximum energy conversion from human motion using piezoelectric flex transducer: A multi-level surrogate modeling strategy, *J. Intell. Mater. Syst. Struct.*, **29**(2018), no, 15, 3097–3107. DOI: 10.1177/1045389X18783075

[14] S.Guo, W.Li, L.Sang, C.Sun, X.Z.Zhao, Finite element analysis of underwater cymbal transducers with large displacement and fast response time, *Integr. Ferroelectr.*, **78**(2006), no. 1, 103–111. DOI: 10.1080/10584580600660025

[15] J.Y.Pyun, Y.H.Kim, K.K.Park, Design of piezoelectric acoustic transducers for underwater applications, *Sensors*, **23**(2023), 1821. DOI: 10.3390/s23041821

[16] A.V.Nasedkin, A.A.Nasedkina, A. Rajagopal, Analysis of cymbal transducer from porous piezoceramics PZT-4 with various material properties based on ANSYS, *Advanced Materials. Springer Proceedings in Physics*, **207**(2018), 533–547. DOI: 10.1007/978-3-319-78919-4_42

[17] A.V.Nasedkin, A.A.Nasedkina, M.E.Nassar, Finite element calculation of disk transducer with cymbal-shaped end-caps and active element from porous piezoceramics with extreme conductivity of pore surfaces, *Problems of Strength and Plasticity*, **85**(2023), no. 1, 63–76 (in Russian). DOI: 10.32326/1814-9146-2023-85-1-63-76

[18] A.V.Nasedkin, A.A.Nasedkina, M.E.Nassar, Finite element investigation of disk transducers from porous piezoceramics of complex structure with cymbal end-caps in external medium, 2023 Days on Diffraction (DD), St. Petersburg, Russia, IEEE Publ., 2023, 156–161. DOI: 10.1109/DD58728.2023.10325699

[19] A.V.Nasedkin, A.A.Nasedkina, Y.V.Tolmacheva, Computer homogenization of porous piezoceramics of different ferrohardness with random porous structure and inhomogeneous polarization field, *Comput. Contin. Mech.*, **16**(2023), no. 4, 476–492 (in Russian). DOI: 10.7242/1999-6691/2023.16.4.40

[20] E.Dieulesaint, D.Royer, Elastic Waves in Solids: Application to Signal Processing, J.Wiley, New York, 1980.

Анализ влияния пористости и неоднородной поляризации пьезокерамики на эффективность мостового преобразователя как сенсора и актуатора

Андрей В. Наседкин
Анна А. Наседкина
Южный федеральный университет
Ростов-на-Дону, Российская Федерация

Аннотация. Гибкие пьезоэлектрические преобразователи с мостовыми накладками нашли широкие применения в качестве акустических излучателей и устройств накопления энергии. В настоящей работы исследуются возможности использования пористой пьезокерамики в качестве активного элемента мостового преобразователя. Особое внимание уделяется учету неоднородности поляризации пористой пьезокерамики с применением упрощенных моделей, пригодных для практики. Проведен конечно-элементный анализ работы мостового пьезопреобразователя при установившихся колебаниях в нерезонансных и в резонансных режимах его работы. Было установлено, что использование пористой пьезокерамики повышает эффективность преобразователя при колебаниях вблизи первой частоты электрического антирезонанса.

Ключевые слова: электроупругость, мостовой пьезопреобразователь, пористая пьезокерамика, неравномерная поляризация, резонансная частота, сенсор, актуатор, метод конечных элементов.